



**Mechanistic analysis of ammonium cation stability for
alkaline exchange membrane fuel cells**

Journal:	<i>Journal of Materials Chemistry A</i>
Manuscript ID:	TA-ART-06-2014-003300.R1
Article Type:	Paper
Date Submitted by the Author:	23-Jul-2014
Complete List of Authors:	Mohanty, Angela; Rensselaer Polytechnic Institute, Chemistry & Chemical Biology Bae, Chulsung; Rensselaer Polytechnic Institute, Chemistry & Chemical Biology

Cite this: DOI: 10.1039/c0xx00000x

Article Type

www.rsc.org/xxxxxx

Mechanistic analysis of ammonium cation stability for alkaline exchange membrane fuel cells†

Angela D. Mohanty and Chulsung Bae*

Received (in XXX, XXX) Xth XXXXXXXXX 20XX, Accepted Xth XXXXXXXXX 20XX

DOI: 10.1039/b000000x

Improving long-term cation stability is crucial for adopting anion exchange membrane fuel cells as a commercially viable technology in clean energy conversion applications. To reliably identify the most stable cation structures, we analyzed the cation stability of various synthetically prepared quaternary ammonium organic molecules via a silver oxide ion exchange reaction. This method enabled us to compare the stability of various structures of quaternary ammonium hydroxide in pure form in water without excess alkaline solution or inconsistencies faced in the presence of polymer backbones. By quantitatively comparing cation degradation via NMR, we were able to identify three cation structures with greater cation stability than the most well-known benzyltrimethylammonium. In addition, we were able to elucidate byproduct formation and degradation mechanisms as a result of hydroxide attack. From this study we concluded that alkyl-substituted cations seem to impart greater stability than benzylic-substituted cations in the presence of hydroxide anion in aqueous solution.

15

1. Introduction

Fuel cells are an attractive clean energy conversion technology since they convert the chemical energy stored in fuels directly and efficiently into electrical energy without emission of polluting chemicals.^{1,2} Among ion-conducting solid electrolyte fuel cells, anion exchange membrane (AEM) fuel cells have recently gained significant attention as a viable technology that can overcome the limitations of proton exchange membrane (PEM) fuel cells because of benefits of (a) facilitated oxygen reduction kinetics in an alkaline environment; (b) efficient water management; (c) flexibility in choices of fuels; (d) the use of inexpensive, non-precious metal electrocatalysts (e.g., nickel).³ In AEM fuel cells, hydroxide ions are transported from the cathode to the anode across a solid alkaline electrolyte, and water is consumed at the cathode as a part of oxygen reduction reaction. The most challenging technical hurdle for adoption of AEM fuel cells is lack of membrane materials that have high hydroxide conductivity and long-term stability under high pH conditions.^{3,4} Unlike Nafion in PEM fuel cells, a state-of-the-art membrane material for AEM fuel cells has yet to be developed.

Although AEM chemical degradation has been widely acknowledged in literature, consistent and systematic studies of the stability of various cations are not available. The majority of AEM stability studies compare chemical degradation of the cationic species that are tethered to a polymer backbone and monitor the chemical stability with changes in FT-Raman, ion-exchange capacity (IEC) and ionic conductivity of the membranes as a function of time in various concentrations of alkaline solutions.⁵⁻⁹ These experimental methods have created inconsistencies in comparing cation stability because different

stability of polymer backbones may play a significant role in the overall AEM stability,¹⁰ and changes in IEC and ionic conductivity may not truly represent chemical degradation by OH⁻ anion. Some investigations into the stability of small molecule organic cations in the presence of alkaline solutions have been reported, but they are unfortunately limited in substrate scope or testing methodology.¹¹⁻¹⁵ Recently NMR spectroscopy has been recognized as a powerful tool for characterization of degradation products and quantitative analysis.^{10,16,17}

Herein we report a straightforward method to assess the cation stability of AEMs by designing an experiment that can compare the stability of various cation species in water directly, quantitatively, and systematically using NMR spectroscopic methods. To eliminate inconsistencies derived from the degradation of polymer backbones, we synthesized small molecule model compounds bearing various quaternary ammonium (QA) halides and converted their counter anions to hydroxide ion in deuterated water (D₂O) by ion exchange reactions with silver oxide (Ag₂O). This synthetic strategy allows convenient preparation of a variety of structures of QA hydroxide (or deuteroxide) in pure form in D₂O and quantitative study of QA degradation by ¹H NMR spectroscopy analysis. Additionally, byproduct analysis with gas chromatography-mass spectrometry (GC-MS) and two-dimensional (2D) NMR yielded further insights into possible mechanisms of cationic degradation.

2. Experimental

2a. General experimental details

Unless otherwise noted, all reagents were purchased from Alfa Aesar, Acros Organics, or Sigma Aldrich and were used without further purification. Anhydrous tetrahydrofuran (THF) was

obtained from Acros Organics and stored in a nitrogen-filled glovebox. Deuterated chloroform (CDCl_3) and deuterium oxide (D_2O) were purchased from Cambridge Isotope Laboratories, Inc.

All synthetic reactions were conducted in vials fitted with Teflon-lined screw cap under air unless otherwise noted. Reactions for benzylamine synthesis were monitored by thin-layer chromatography (TLC) using Baker-flex silica gel IB-F (2.5 x 7.5 cm) plates and were visualized by UV light. Flash column chromatography was performed with silica gel 60 (70-230 mesh ASTM).

^1H NMR spectra were obtained with a Varian Unity 500 MHz spectrometer. ^{13}C and 2D-NMR spectra were obtained with a Bruker 600 MHz (14.1 Tesla) spectrometer. All NMR spectra were recorded at 25 °C and chemical shifts were referenced to solvent residue peak of CDCl_3 (at 7.26 ppm) or 18-crown-6 ether internal standard (at 3.70 ppm in D_2O) and were recorded using 5 second relaxation delay. NMR spectra were processed with MestReNova 8.1 (Mestrelab Research SL) software. GC-MS analysis was conducted with a Shimadzu GC-2010 equipped with a ZB-XLB column (30 m x 0.25mm ID x 0.25 μm film) and a Shimadzu GC-MS-QP2010S detector. The temperature for each run was ramped from 40 to 250 °C at 20 °C/min, and then held at 250 °C for 40 min.

2b. General procedure for preparation of amines

The following represents a typical procedure for synthesis of *N,N*-dimethylbenzylamine from benzyl bromide. A 40 mL vial containing dioxane (10 mL) and benzyl bromide (5.00 g, 29.2 mmol) was cooled in an ice bath. Dimethylamine solution (40 wt% in H_2O , 5.9 mL, 117 mmol) was slowly added. After stirring in the ice bath for 2 h, the reaction was quenched with 0.5 M NaHCO_3 (10 mL) and water (10 mL), and extracted with diethyl ether (4 x 25 mL). The organic layer was dried over MgSO_4 , filtered, and concentrated on a rotary evaporator to yield a colorless liquid (0.61 g, 15 % yield).

2c. General procedure for methylation of amines

To a 20 mL vial was added a synthetically prepared benzylamine (1 mmol, 1 equiv) and dichloromethane (1 mL per mmol of amine). Chilled methyl iodide (3 mmol, 3 equiv based on amine) was added all at once. The reaction was stirred at rt for a specified amount of time (see supporting information, ESI†). On completion of the reaction, the resulting white precipitate was filtered and rinsed with cold dichloromethane (3 x 5 mL), unless otherwise noted. The quaternized benzylammonium iodide was collected and vacuum dried.

2d. General procedure for stability analysis via Ag_2O ion exchange reaction

To a 5 mL vial was added synthetically prepared benzylammonium halide (0.1 g, 1 equiv) and D_2O (1.5 mL). To this vial was added silver oxide (Ag_2O , 0.13 g, 1.5 equiv). After stirring at rt for 3 h, the reaction mixture was centrifuged for 10 min to precipitate the silver halide solids and unreacted silver oxide. The top solution was removed and filtered through a tightly packed cotton plug into a vial. [Note: Filtration was sufficient for complete removal of the silver halide precipitates and unreacted Ag_2O solids. Because a slight excess of Ag_2O was used (to facilitate complete ion exchange), a small amount of the

Ag_2O could remain solubilised in the QA deuteroxide solutions. However, since the solubility of Ag_2O in water at 25 °C is only 0.025 mg/mL,¹⁸ the maximum solubilised Ag_2O concentration after filtration would be 1×10^{-4} mmol/mL which is far below the concentration of QA (approximately 0.24 mmol). Thus, it is unlikely that the remaining dissolved Ag_2O influences cation degradation.] To this vial was added 1 drop of 18-crown-6 solution (0.45 M in D_2O), then 0.45 mL of this solution was transferred to a NMR tube which was capped and sealed with parafilm. ^1H NMR spectrum was immediately recorded (labelled as 0 h) and then the NMR tube was placed in an oil bath set at a specified temperature (60 and 120 °C). NMR spectra were recorded at specified time intervals of 24, 144, 264, 432, and 672 h.

2e. General procedure for byproduct analysis

At the end of the stability study (i.e., after 672 h), QA in D_2O solution was transferred to a 5 mL vial. Neutral organic byproducts were extracted with CDCl_3 (1 mL). The CDCl_3 layer was separated from the D_2O layer and the organic extracts were analyzed with GC-MS, ^1H -, ^{13}C -, and 2D-NMR without further workup procedures.

3. Results and discussion

3a. QA-model compounds of this study

The QA-model compounds prepared for this stability study are shown in Figure 1a. All QAs except for **TMHA** were attached at the benzylic position to an aromatic ring to mimic the most commonly studied QA moieties tethered to aromatic polymers in AEM literature. We also designed several QA structures that contain β -hydrogen but the cation centers are sterically hindered to suppress OH^- attack. These examples include **MnPr**, **MiPr**, **MCH**, **DABCO-1**, and **DABCO-2**. Of these, **MiPr** has the most accessible β -hydrogen at primary carbon which can undergo Hofmann elimination when attacked by hydroxide anion. **MnPr**, **DABCO-1**, and **DABCO-2** have β -hydrogen as well, but they are attached to more sterically hindered secondary carbons. Because hydroxide ion tends to abstract β -hydrogen preferentially at sterically less-hindered carbons in Hofmann elimination, we postulated that it would be less likely to occur in these QA-model compounds. For **MCH**, in spite of having β -hydrogen, Hofmann elimination will be difficult because it requires the anti-coplanar position (180° dihedral angle) of the two eliminating groups (i.e., β -hydrogen and ammonium cation in trans-diaxial geometry) while the bulky ammonium group prefers being in the equatorial position of the cyclohexane rings. Resonance stabilized cations such as guanidinium (**TMG**), imidazolium (**1,2-DMIm**), and pyridinium (**Pyr**, **2MPyr**) and cations bearing long alkyl chains such as **DMHA** and **TMHA** were also included in this study since they have recently gained attention in AEM literature.^{6,11,12,19} Benzyltrimethylammonium (**TMA**) was used as the base QA for comparison with all model compounds because it is the most widely used QA structure in AEM materials.

Ion exchange reaction of halide anions to OH^- (or OD^-) was conducted with Ag_2O in D_2O (Figure 1b) where the resulting silver halides precipitated from the solution. The primary reason for choosing this method of ion exchange over the commonly

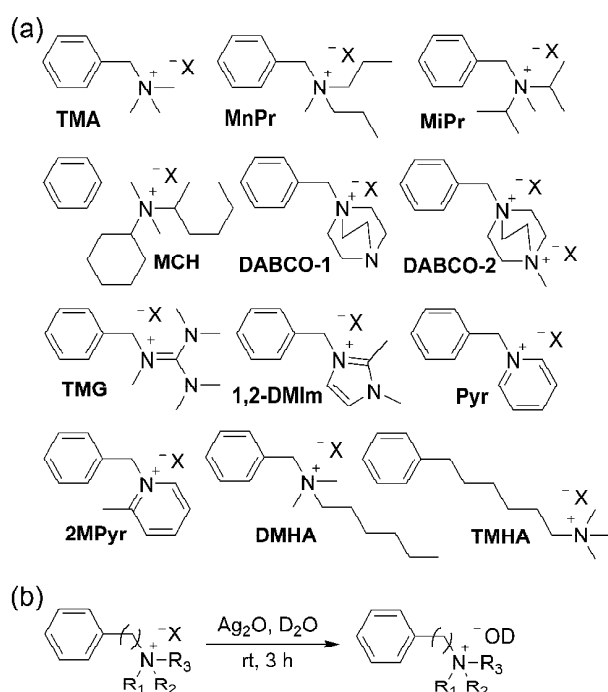


Fig. 1 (a) Quaternary ammonium-model compounds prepared for alkaline stability study, where $\text{X} = \text{Br}$ or I . (b) Ag_2O -mediated ion exchange reaction.

used ion exchange reaction with sodium hydroxide was that some QA-model compounds exhibited poor solubility in aqueous NaOH solution whereas all model compounds were fully soluble in pure water (or D_2O). Some researchers have reported stability measurements of QAs in a mixture of methanol and water solutions to increase solubility.^{10,12,20} However, we wanted to avoid adding methanol since it can change the polarity of reaction medium and affect the reactivity of hydroxide anion toward QAs. A major advantage of using Ag_2O -mediated ion exchange reaction is that it allows isolation of QAs of Figure 1a in pure form without contamination of undesired species (e.g. unreacted amines, unexchanged halide anion, excess NaOH) and the examination of their cation degradation solely by the accompanying hydroxide (or deuteroxide) anion. Once they were prepared, we were able to monitor QA degradation caused by OH^- (or OD^-) conveniently and accurately via NMR. Although we prepared QAs in OD^- form in Figure 1b because the reaction solvent was D_2O , deuteroxide would have the same degradation effect as hydroxide does in H_2O . D_2O typically contains a significant amount of H_2O . Thus, we will use OD^- and OH^- interchangeably throughout this report. During the course of this study, it was discovered that Ag_2O -mediated ion exchange reaction of 1-methyl-3-benzylimidazolium bromide formed *N*-heterocyclic carbene-Ag complex possibly due to the presence of acidic hydrogen at C-2 of imidazolium ion.²¹ Instead, **1,2-DMIm** in which the acidic hydrogen is replaced by methyl was used instead for this study. It has been shown that insertion of methyl group at C-2 position of imidazolium can improve its stability.^{11,22,23}

An internal standard (18-crown-6) was added to the QA-containing D_2O solutions. We chose 18-crown-6 as the most suitable internal standard because (a) it has a high boiling point

thus eliminating possibility of evaporation, (b) it produces a single resonance in ^1H and ^{13}C NMR spectra that does not overlap with resonances of the model compounds, (c) it is readily soluble in D_2O , and (d) it is chemically stable even in high pH conditions at elevated temperature. The solutions were transferred to tightly sealed NMR tubes and heated to 60 and 120 $^\circ\text{C}$. NMR spectra were recorded at time intervals of 0, 24, 144, 264, 432, and 672 hours. The solutions were never removed from the NMR tubes throughout the entire study so as to not disturb or lose any compounds contained within the solution mixture. Cation degradation was quantitatively determined by monitoring changes in the integral ratio of NMR resonance peaks of model compounds as compared to that of the internal standard 18-crown-6 resonance at 3.70 ppm (set to an integral ratio of 1.0). NMR spectra of each investigated QA-model compound can be found in Figures S14-S31 in ESI†.

3c. Comparison of QA-model compound cation stability

The studied QAs exhibited broad ranges of stability; some degraded fast at 60 $^\circ\text{C}$, whereas others were quite stable up to 120 $^\circ\text{C}$. Therefore, the QAs were divided into two groups based on their thermochemical stability. The less stable group QA-model compounds were investigated at 60 $^\circ\text{C}$ (**DABCO-2**, **TMG**, **1,2-DMIm**, **Pyr**, and **2MPyr** seen in Figure 2a) while the more stable QA structures were investigated at a higher temperature 120 $^\circ\text{C}$ to accelerate degradation conditions (**MnPr**, **MiPr**, **MCH**, **DMHA**, and **TMHA** seen in Figure 2b). **TMA** was investigated at both temperatures so that its stability can be used as the reference to all model compounds. **DABCO-1** was initially tested at the lower temperature for direct comparison with **DABCO-2**, but was found to be stable at 60 $^\circ\text{C}$. Therefore, **DABCO-1** was included in the 120 $^\circ\text{C}$ study as well.

As evidenced in Figure 2a, **DABCO-2** is the least stable QA. The inferior alkaline stability of bis-QAs (e.g., **DABCO-2**) as compared to mono-QAs (e.g., **DABCO-1**) seems to be in agreement with literature observations.¹³ Recently resonance-stabilized cation structures (e.g., **TMG**, **1,2-DMIm**, **Pyr**, **2MPyr** of Figure 1a) have gained increased attention in AEM materials because they are believed to have reduced susceptibility toward hydroxide nucleophilic attack due to their delocalized cation structures.^{11,12,19,24} However, our results indicate that all these benzylic-substituted resonance-stabilized cations possess poor cation stability in the presence of OD^- in comparison to **TMA** (Figure 2a). Introducing a methyl group next to positive nitrogen of imidazolium and pyridinium (i.e., **1,2-DMIm** and **2MPyr**) can enhance steric hindrance and improve the stability compared to non-methylated counterparts. Nevertheless, the chemical stabilities of **1,2-DMIm** and **2MPyr** were not as good as **TMA**.

Extra caution was taken when analyzing the degradation of imidazolium and pyridinium model compounds with NMR spectroscopy since they contain acidic hydrogen that readily undergo hydrogen-deuterium exchange in the presence of $\text{OD}^-/\text{D}_2\text{O}$ solution.^{25,26} For example, the proton NMR signals of benzylic carbon and C-2 position of pyridinium ring in **Pyr** disappeared within 24 h (see peaks b and c in Figure S24 in ESI†). To confirm that the disappearance of these NMR signals was due to H/D exchange and not degradation, we analyzed **1,2-DMIm**, **Pyr**, and **2MPyr** with ^{13}C NMR (see Figures S23, S25, and S27 in ESI†). All ^{13}C NMR resonances were visible at 0 h,

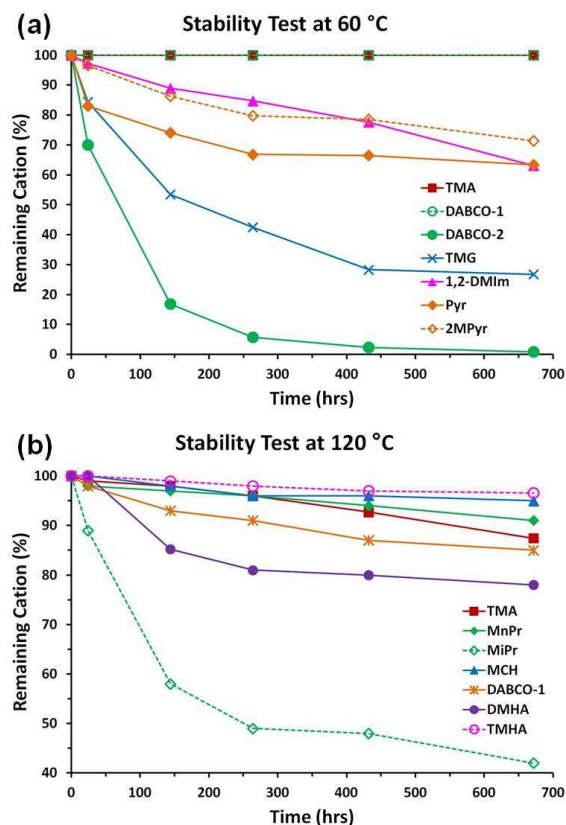


Fig. 2 Percentage of remaining cation over time at (a) 60 °C for **TMA**, **DABCO-1**, **DABCO-2**, **TMG**, **1,2-DMIm**, **Pyr**, and **2MPyr** [Note: **TMA** and **DABCO-1** data sets overlap at 100% remaining cation]; and (b) 120 °C for **TMA**, **MnPr**, **MiPr**, **MCH**, **DABCO-1**, **DMHA**, and **TMHA**.

but changes were observed after heating for only 24 h. For **Pyr**, after 24 h at 60 °C the ^{13}C NMR signals of the benzylic carbon and the aromatic carbon next to N of pyridinium became split and their intensities significantly decreased (see peaks 5 and 6 of Figure S25 in ESI †). We confirmed that the splitting patterns observed for these peaks are consistent with splitting that could occur from C-D coupling.^{22,27} Because deuterium has a spin of 1, the resonance for C-6 of pyridinium (centered at 145.0 ppm with a coupling constant $J_{\text{C-D}} = 30.1$ Hz) appeared as a 1:1:1 triplet because it coupled with one deuterium. The ^{13}C NMR resonance of benzylic carbon (centered at 65.2 ppm with $J_{\text{C-D}} = 21.4$ Hz) also appeared as a quintet due to its coupling with two deuteriums. When the same NMR sample was analyzed with deuterium-decoupled ^{13}C NMR, those two ^{13}C signals regained singlets (see Figure S25c in ESI †). Since the rapid H/D exchanges made it difficult to calculate cation degradation of **1,2-DMIm**, **Pyr**, and **2MPyr**, the changes in integral ratios of non-exchangeable aromatic protons were used to calculate percentage of remaining cation.

We also conducted cation degradation of **Pyr** in a 5% $\text{D}_2\text{O}/\text{H}_2\text{O}$ solution to reduce H/D exchange. Consequently, the resonance intensity of acidic hydrogens decreased to a lesser extent as compared with that of pure D_2O (Figure S34 in ESI †). In 5% D_2O solution the resulting anion was mostly in OH^- form,

whereas in 100% D_2O solution the anion exists as OD^- . As seen in Figure S33 in ESI † , both 5% and 100% D_2O solutions resulted in a similar degradation rate for **Pyr**, suggesting that OH^- and OD^- have the same effect on cation degradation. Degradation of **Pyr** with Br^- counter anion was also investigated (see Figure S33 in ESI †) and was found that it did not suffer any loss of cationic group. This confirms that the method of Ag_2O -mediated ion exchange reaction successfully yielded the QA structure in the desired OH^- (or OD^-) form.

To facilitate a faster degradation study within a reasonable time frame, we analyzed the more stable QA-model compounds at a higher temperature 120 °C (Figure 2b). Increasing temperature to 120 °C resulted in mild reflux of D_2O in the NMR tubes, but no reduction in solvent volume was observed, thus all QAs remained fully solvated. Among seven model compounds of the more stable QA group, three compounds (**DABCO-1**, **MiPr**, and **DMHA**) were found to have lower or a similar stability as compared to **TMA**, while three (**MnPr**, **MCH**, and **TMHA**) showed better stability than **TMA**.

The alkaline stability of **TMHA** stands out among all QA-model compounds tested; it remained the most stable throughout the entire 120 °C stability test. Thus, we further investigated the alkaline stability of **TMHA** at 140 °C. This degradation study was conducted in a sealed vial rather than directly in NMR tube. When the vial was placed in a 140 °C oil bath it was noticed that D_2O boiled immediately and condensed on the upper wall of the glass vial. The reduced volume of liquid at the bottom of the vial might have resulted in less solvation around the cation and accelerated OD^- attack, causing a significant amount of precipitate formation. **TMHA** stability was also investigated with excess of hydroxide ion in solution. Since the solubility of **TMHA** in 2M $\text{NaOD}/\text{D}_2\text{O}$ was poor, we investigated its stability in a 2M $\text{NaOD}/\text{CD}_3\text{OD}$ solution. Surprisingly, **TMHA** remained relatively stable even in this concentrated alkaline solution, having 66% remaining cation after 672 h at 90 °C (Figure S32 in ESI †). These results demonstrate exceptional stability of **TMHA** in high pH environments. This also indicates that the use of excess hydroxide in solution does accelerate the rate of cation degradation in comparison to the Ag_2O -mediated ion exchange reactions. However, a direct stability comparison between 2M $\text{NaOD}/\text{CD}_3\text{OD}$ solution test and QAs in pure OD^- form cannot be made since methanol could have changed the polarity of solution and likely affected the reactivity of deuteroxide toward **TMHA**.

3d. Isolation and analysis of byproducts

Throughout the degradation study we discovered that byproducts from alkaline degradation of QAs were not always observed in the NMR spectral data because some of these byproducts were insoluble in D_2O . This was evidenced by visual observation of precipitate formation and color changes in many of the NMR tubes (Figures S35-S36 in ESI †) but no additional new peaks in NMR spectra. To gain more detailed structure information of the insoluble byproducts and more insightful degradation analysis of QAs, we extracted these organic byproducts with CDCl_3 from the D_2O solution and analyzed with GC-MS, ^1H -, ^{13}C - and 2D-NMR spectroscopies without further workup procedures (Figures S37-S48 in ESI †).

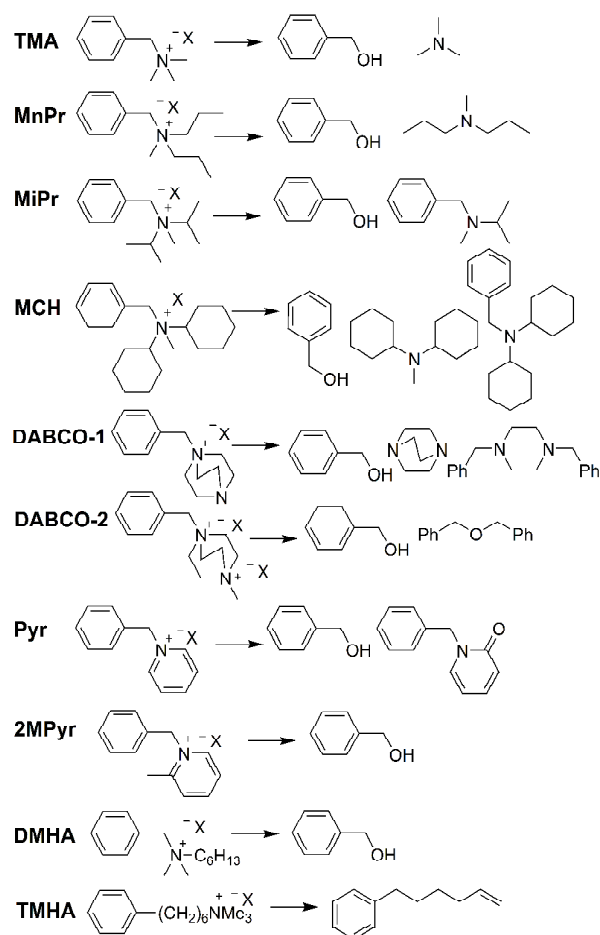


Fig. 3 Byproducts identified from CDCl_3 extraction after cation degradation studies (where X = OH or OD).

Figure 3 lists byproducts that were identified from cation degradation of each model QA investigated. Byproducts of **TMG** and **1,2-DMIm** were unable to be identified presumably as a result of rearrangements of initially formed degradation byproducts. Nevertheless, it was apparent that benzyl alcohol was the most commonly formed byproduct [structure determination of benzyl alcohol was confirmed by comparing with spectroscopic data of authentic sample of benzyl alcohol (Figure S13 in ESI†)]. This observation suggests that the benzylic position of benzyl-substituted QAs is the weakest position at which degradation will most likely occur. If we compare the degradation of **DMHA** and **TMHA**, a pair of isomeric QAs containing *n*-hexyl chains, **TMHA** showed better cation stability than **DMHA** (97% vs. 78% remaining cations at 120 °C). Similar trends were reported in AEM literature, in which it's been stated that the benzylic carbon may undergo facile $\text{S}_{\text{N}}2$ attack by OH^- as a result of the electron-withdrawing inductive and resonance effects of the aromatic ring (e.g., as in **DMHA**) in comparison to an aliphatic chain (e.g., **TMHA**).^{6,7} Benzyl alcohol byproduct was not observed for **TMHA**, the only identified byproduct from the 140 °C study was a Hofmann elimination product which resulted from the loss of trimethylamine. As suggested by computational studies,²⁸ it appears that the stability of alkyltrimethylammonium cation bearing β -hydrogens is dependent on the structure of alkyl chain, the structure around β -hydrogen susceptible to Hofmann

elimination, and degradation conditions. For example, when degradation of *n*-propyltrimethylammonium hydroxide was studied *under dry condition* with evolved gas analysis, Boncella and co-workers reported the degradation occurred at much lower temperature (below 50 °C) and the Hofmann elimination was the primary decomposition pathway.¹⁵ However, our data suggests that the Hofmann elimination of a long alkyltrimethylammonium hydroxide, although it is the main degradation pathway as in **TMHA**, needs to overcome a large activation energy barrier and requires temperature >100 °C *under fully hydrated conditions*.

Byproduct analysis of **MCH** suggests hydroxide ion attack occurred both at the benzylic carbon and at the *N*-methyl. The enhanced stability of **MCH** in comparison to **TMA** likely results from its large cyclohexane rings that shield the benzylic carbon from OD^- attack via steric hindrance. As mentioned, Hofmann elimination is difficult to occur in **MCH** because of the requirement of anti-coplanar geometry of β -hydrogen and the bulky nitrogen cation group.

3e. Mechanistic analysis of degradation

It is interesting to note the differences in alkaline stability between **MnPr** and **MiPr**. The former QA with linear alkyl chains showed significantly better alkaline stability than the latter one with branched chains (91% vs. 42% remaining cations at 120 °C, Figure 2b). Based on byproduct analysis of Figure 3, it was found that OH^- attack occurred at the benzylic carbon for both **MnPr** and **MiPr** thus forming benzylic alcohol as a byproduct. In **MiPr**, however, OH^- also attacks the isopropyl chains forming benzylisopropylmethylamine by E2 Hofmann degradation (mechanism shown in Figure 4b). The formation of benzylisopropylmethylamine byproduct via OH^- attack at the C-2 carbon of the isopropyl moiety is not feasible due to greater steric hindrance of the isopropyl group. A Hofmann elimination byproduct was not observed for **MnPr** under the identical condition. Although both QAs contain β -hydrogen, the hydroxide ion seems to attack the less hindered β -hydrogen preferentially causing Hofmann elimination in the branched isopropyl chains but not in linear *n*-alkyl chains. The availability of this additional degradation pathway of **MiPr** might have caused the faster degradation rate.

The major identifiable byproducts from **TMA** degradation were benzyl alcohol and trimethylamine. These organic byproducts can be formed by nucleophilic attack of OH^- (or OD^-) at the benzylic carbon ($\text{S}_{\text{N}}2$ of Figure 4a and $\text{S}_{\text{N}}2$ -d of Figure 4c) and reaction of water with nitrogen ylide that was formed by abstraction of α -hydrogen at the benzylic carbon (Figure 4c, Ylide II route). Although the contribution of nitrogen ylide mechanism for degradation of tetraalkylammonium hydroxide has been recognized by experimental and computational studies,^{29,30} the degradation experiment was conducted only under dry conditions so far.^{15,31} Direct nucleophilic attack of OH^- (or OD^-) at the benzylic carbon of **TMA** ($\text{S}_{\text{N}}2$ of Figure 4a) will afford $\text{C}_6\text{H}_5\text{-CH}_2\text{OH}$ (or $\text{C}_6\text{H}_5\text{-CH}_2\text{OD}$). When we analyzed the MS of benzyl alcohol degradation byproduct, however, we found that more than one deuterium has been incorporated giving molar masses of heavier mass isotopomers of benzyl alcohol (refer to Figure 5c). This result suggests that $\text{S}_{\text{N}}2$ route of Figure 4a is not the sole source of degradation mechanism: the benzyl alcohol byproduct was also formed via the reaction of D_2O with Ylide II

and/or S_N2 -d route of Figure 4c. Please note these two degradation pathways of Figure 4c involve the same Ylide II

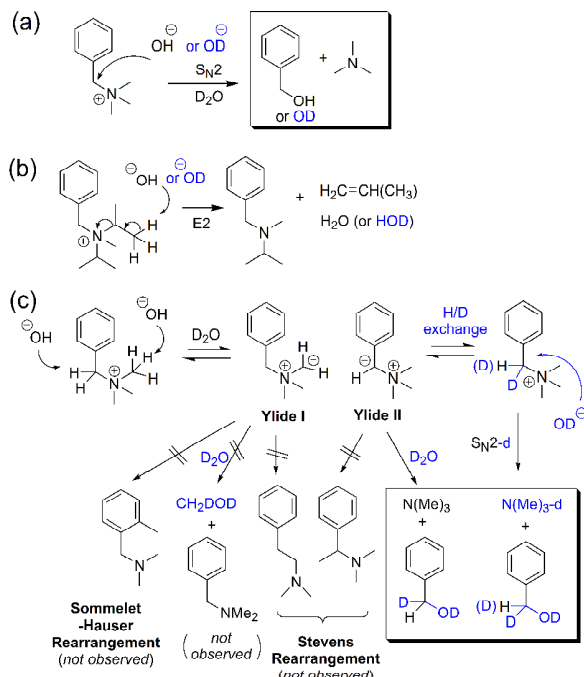


Fig. 4 Possible routes of QA cation degradation via hydroxide (or deuterioxide) attack; (a) nucleophilic S_N2 displacement, (b) Hofmann E2 elimination if β -hydrogen are available, (c) reversible ylide formation via hydroxide attack at α -hydrogen, which may further undergo irreversible degradation or rearrangements.

intermediate, which can (i) undergo a rapid reversible H/D exchange reaction followed by nucleophilic attack of hydroxide ion in S_N2 -d route or (ii) react with D_2O directly to give deuterated benzyl alcohol. Distinguishing these two routes will be difficult because both would give the same product. Nevertheless, this deuterium scrambling result clearly supports that Ylide II is an intermediate in thermochemical degradation of **TMA**. We think decomposition of **TMA** via Ylide I route is an unlikely pathway because we did not detect *N,N*-dimethylbenzylamine and any rearrangement byproducts (Sommerlet-Hauser and Stevens Rearrangements).

MS data of benzyl alcohol byproducts from other QAs also suggests that both S_N2 and ylide degradation are responsible for benzyl alcohol formation. Although more mechanistic studies will be required, it is generally observed that the less stable QAs (e.g., **DABCO-2** in Figure 5d) showed a lesser extent of deuterium incorporation via ylide, suggesting more contribution of S_N2 pathway to the degradation (see Figure S49 in ESI† for all MS data).

4. Conclusions

In summary, we were able to assess the alkaline stability of various cation structures in pure OH^- (or OD^-) form by utilizing a straightforward Ag_2O -mediated ion exchange reaction. From quantitative NMR analysis, we identified three cation structures with greater alkaline stability (**MnPr**, **MCH**, and **TMHA**) in

comparison to the well-known **TMA**. We also identified two QA-model compounds with comparable stability (**DABCO-1** and

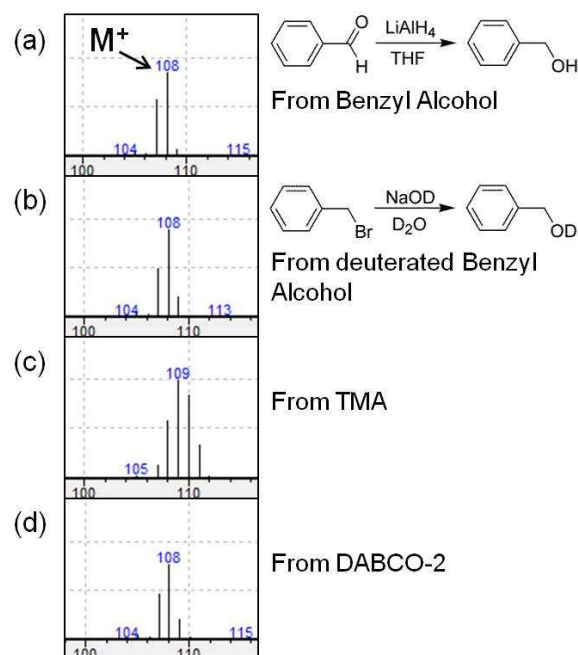


Fig. 5 MS spectra of selected benzyl alcohol byproducts and their comparison with authentic samples.

DMHA) and six compounds with poorer cation stability (**DABCO-2**, **TMG**, **1,2-DMIm**, **Pyr**, **2MPyr**, and **MiPr**) than **TMA**. From the observation of significant formation of benzylic-substituted byproducts, we conclude that AEM materials functionalized with benzylic-substituted cation moieties will most likely be insufficient for long-term alkaline stability. We believe alkyl-substituted cation moieties are possibly the best QA candidates that can provide long-term alkaline stability for AEM materials.

Although cation degradation in polymeric membrane was not investigated in this report, we postulate that stability trends observed in this small molecule study would follow similar stability trends in polymer membrane form, as observed in other literature reports.^{5,12,20} However, AEM materials with hindered cations may exhibit low hydroxide conductivity because of increased hydrophobicity around the cation and the resulting lower water uptake. Ongoing work in our group includes incorporation of these QA structures to polymer backbones and investigation of their stability and membrane properties. Development and stability analysis of such novel AEM materials will be disclosed in future publications.

Acknowledgements

Financial support from NSF CAREER Award (CB) and Rensselaer Polytechnic Institute is greatly appreciated.

Notes and references

⁵⁵ Department of Chemistry and Chemical Biology, Rensselaer Polytechnic Institute, 110 8th Street, Troy, NY 12180. Tel: 1-518-276-3783; E-mail: baec@rpi.edu

- † Electronic Supplementary Information (ESI) available: [Detailed synthetic procedures; NMR spectra for all model compounds; preparation and analysis of benzyl alcohol; high temperature and concentrated alkaline degradation study for **TMHA**; **Pyr** degradation analysis in 5% D₂O; NMR spectra of all degradation experiments; ¹³C NMR for **1,2-DMIm**, **Pyr**, and **2MPyr**; photos of imidazolium and pyridinium color changes; GC-MS and NMR spectra for isolated byproducts]. See DOI: 10.1039/b000000x/
- 1 G. Couture, A. Alaaeddine, F. Boschet and B. Ameduri, *Prog. Polym. Sci.*, 2011, **36**, 1521-1557.
- 2 G. Merle, M. Wessling and K. Nijmeijer, *J. Membr. Sci.*, 2011, **377**, 1-35.
- 3 J. R. Varcoe and R. C. T. Slade, *Fuel Cells*, 2005, **5**, 187-200.
- 4 Y. Yuesheng and A. E. Yossef, in *Polymers for Energy Storage and Delivery: Polyelectrolytes for Batteries and Fuel Cells*, American Chemical Society, 2012, vol. 1096, pp. 233-251.
- 5 O. I. Deavin, S. Murphy, A. L. Ong, S. D. Poynton, R. Zeng, H. Herman and J. R. Varcoe, *Energy Environ. Sci.*, 2012, **5**, 8584-8597.
- 6 M. R. Hibbs, *J. Polym. Sci., Part B: Polym. Phys.*, 2013, **51**, 1736-1742.
- 7 M. Tomoi, K. Yamaguchi, R. Ando, Y. Kantake, Y. Aosaki and H. Kubota, *J. Appl. Polym. Sci.*, 1997, **64**, 1161-1167.
- 8 C. G. Arges, J. Parrondo, G. Johnson, A. Nadhan and V. Ramani, *J. Mater. Chem.*, 2012, **22**, 3733-3744.
- 9 T. Sata, M. Tsujimoto, T. Yamaguchi and K. Matsusaki, *J. Membr. Sci.*, 1996, **112**, 161-170.
- 10 S. A. Nuñez and M. A. Hickner, *ACS Macro Lett.*, 2012, **2**, 49-52.
- 11 S. C. Price, K. S. Williams and F. L. Beyer, *ACS Macro Lett.*, 2014, 160-165.
- 12 F. Gu, H. Dong, Y. Li, Z. Si and F. Yan, *Macromolecules*, 2013, **47**, 208-216.
- 13 B. Bauer, H. Strathmann and F. Effenberger, *Desalination*, 1990, **79**, 125-144.
- 14 B. R. Einsla, S. Chempath, L. Pratt, J. Boncella, J. Rau, C. Macomber and B. Pivovar, *ECS Trans.*, 2007, **11**, 1173-1180.
- 15 J. B. Edson, C. S. Macomber, B. S. Pivovar and J. M. Boncella, *J. Membr. Sci.*, 2012, **399**, 49-59.
- 16 C. G. Arges and V. Ramani, *Proceedings of the National Academy of Sciences*, 2013, **110**, 2490-2495.
- 17 C. G. Arges and V. Ramani, *Journal of the Electrochemical Society*, 2013, **160**, F1006-F1021.
- 18 D. R. Lide, in *Handbook of Chemistry and Physics*, CRC Press, Boca Raton, FL, 87 edn., 1998, pp. 4-83.
- 19 D. S. Kim, C. H. Fujimoto, M. R. Hibbs, A. Labouriau, Y.-K. Choe and Y. S. Kim, *Macromolecules*, 2013, **46**, 7826-7833.
- 20 Z. Si, L. Qiu, H. Dong, F. Gu, Y. Li and F. Yan, *ACS Appl. Mater. Interfaces*, 2014, **6**, 4346-4355.
- 21 J. C. Garrison and W. J. Youngs, *Chem. Rev.*, 2005, **105**, 3978-4008.
- 22 B. Lin, H. Dong, Y. Li, Z. Si, F. Gu and F. Yan, *Chem. Mater.*, 2013, **25**, 1858-1867.
- 23 H. Long and B. Pivovar, *J. Phys. Chem. C*, 2014, **118**, 9880-9888.
- 24 J. Wang, S. Li and S. Zhang, *Macromolecules*, 2010, **43**, 3890-3896.
- 25 S. T. Handy and M. Okello, *J. Org. Chem.*, 2005, **70**, 1915-1918.
- 26 J. A. Zoltewicz and C. L. Smith, *J. Am. Chem. Soc.*, 1967, **89**, 3358-3359.
- 27 P. Perrotin, P.-J. Sinnema and P. J. Shapiro, *Organometallics*, 2006, **25**, 2104-2107.
- 28 H. Long, K. Kim and B. S. Pivovar, *J. Phys. Chem. C*, 2012, **116**, 9419-9426.
- 29 S. Chempath, B. R. Einsla, L. R. Pratt, C. S. Macomber, J. M. Boncella, J. A. Rau and B. S. Pivovar, *J. Phys. Chem. C*, 2008, **112**, 3179-3182.
- 30 S. Chempath, J. M. Boncella, L. R. Pratt, N. Henson and B. S. Pivovar, *J. Phys. Chem. C*, 2010, **114**, 11977-11983.
- 31 C. S. Macomber, J. M. Boncella, B. S. Pivovar and J. A. Rau, *J. Therm. Anal. Calorim.*, 2008, **93**, 225-229.